Nucleic Acids Research Advance Access published November 29, 2016

Nucleic Acids Research, 2016 **1**
doi: 10.1093/nar/gkw1178

Chromatin binding of Gcn5 in *Drosophila* is largely mediated by CP190

Tamer Ali[1], Marcus Krüger[2], Sabin Bhuju[3], Michael Jarek[3], Marek Bartkuhn[1] and Rainer Renkawitz[1,*]

[1]Institute for Genetics, Justus-Liebig-University, D35392 Giessen, Germany, [2]CECAD Research Center, University of Cologne, D50931 Cologne, Germany and [3]Helmholtz Centre for Infection Research, D38124 Braunschweig, Germany

Received June 16, 2016; Revised November 04, 2016; Editorial Decision November 11, 2016; Accepted November 17, 2016

ABSTRACT

Centrosomal 190 kDa protein (CP190) is a promoter binding factor, mediates long-range interactions in the context of enhancer-promoter contacts and in chromosomal domain formation. All *Drosophila* insulator proteins bind CP190 suggesting a crucial role in insulator function. CP190 has major effects on chromatin, such as depletion of nucleosomes, high nucleosomal turnover and prevention of heterochromatin expansion. Here, we searched for enzymes, which might be involved in CP190 mediated chromatin changes. Eighty percent of the genomic binding sites of the histone acetyltransferase Gcn5 are colocalizing with CP190 binding. Depletion of CP190 reduces Gcn5 binding to chromatin. Binding dependency was further supported by Gcn5 mediated co-precipitation of CP190. Gcn5 is known to activate transcription by histone acetylation. We used the dCas9 system to target CP190 or Gcn5 to a Polycomb repressed and H3K27me3 marked gene locus. Both, CP190 as well as Gcn5, activate this locus, thus supporting the model that CP190 recruits Gcn5 and thereby activates chromatin.

INTRODUCTION

Insulators are DNA sequences bound by specific proteins that are required to insulate active topologically associated domains (TADs) from adjacent inactive ones or to block enhancers from activating promoters (1). In *Drosophila*, several insulator binding proteins (IBPs), such as dCTCF, Su(Hw), BEAF-32, GAF, ZW5, Ibf1 and 2, Pita and ZIPIC, have been identified and characterized (2–12). These proteins form different complexes by recruiting additional factors such as CP190. It has been shown that CP190 is the essential constituent of the *gypsy* insulator complex together with Su(Hw) and Mod(mdg4)2.2. Among all these DNA-binding insulator factors CP190 binding is shared. Insulator strength is determined by the number of aligned DNA-bound factors (13). It has been shown that two separated domains of CP190 interact with specific IBPs (3), suggesting a bridging role of CP190 allowing clustered IBPs to target CP190 more efficiently. Indeed, synergistic recruitment of CP190 by IBP clusters has been shown (3). Furthermore, insulator function and TAD border strength correlate with IBP protein occupancy (14), suggesting that the efficiency of CP190 binding is an important regulator of CP190 function. In addition to insulator function CP190 has been shown to bind active promoters (15). A unifying chromatin feature for most of the CP190 bound TADs is an increase of histone acetylation at these sites (16).

The histone acetyltransferase Gcn5 is highly conserved, found in yeast as well as in man and is a component of the SAGA complex. A recent *in vitro* study proposed that SAGA binding at active promoters is mediated by the sgf29 Tudor domain binding to H3K4me3 and allowing Gcn5 to acetylate histone H3K9 (17). In human cells, genome-wide ChIP-Seq revealed that Gcn5 is localized at gene promoters (18). Recent analysis of Gcn5 binding in ES cells demonstrated that from the 7000 Gcn5 peaks identified about 50% are located close to the transcriptional start site (TSS) (19). In *Drosophila*, Gcn5 was shown to be dependent on some Su(Hw) insulator sites, which are aligned with origin of replication complexes (20).

Here, we reveal that the recruitment of Gcn5 to chromatin of *Drosophila* is dependent on CP190. Depletion of Gcn5 deregulates a subset of genes that strongly overlap with those deregulated by CP190. Targeted recruitment of Gcn5 or CP190 to silent chromatin resulted in gene activation.

*To whom correspondence should be addressed. Tel: +49 641 9935460; Fax: +49 641 9935469; Email: rainer.renkawitz@gen.bio.uni-giessen.de
Present address: Tamer Ali, Faculty of Science, Benha University, Benha 13518, Egypt.

MATERIALS AND METHODS

Data access

All data sets reported in this study have been submitted to the NCBI Gene Expression Omnibus (GEO; http://www.ncbi.nlm.nih.gov/geo/) under accession number GSE83409.

DNA plasmids and primers

CRISPR/Cas9 plasmid (all in one) was purchased from Addgene (#49330). Wild-type Cas9 was deactivated by site-directed mutagenesis kit (Agilent) using the following primers:

D10A:
FP: 5′-gtacagcatcggcctggctatcggcaccaactctg-3′
RP: 5′-cagagttggtgccgatagccaggccgatgctgtac-3′
H840A:
FP: 5′-gtccgactacgatgtggacgccatcgtgcctcagagctttc-3′
RP:5′-gaaagctctgaggcacgatggcgtccacatcgtagtcggac-3′

dCas9 (D10A and H840A) sequence was validated by sequencing. CP190 and Gcn5 full length cDNA sequences was inserted using HindIII in the reading frame of actin promoter. sgRNA were designed to target a sequence 100 bp upstream of *eve* TSS using crispr.mit.edu web-based tool. The cr-RNA was inserted using the BspQI restriction enzyme.

For other primers see Supplementary Table S3.

Cell culture

Drosophila S2 and Kc cells were maintained in Schneider's media supplemented with 10% FBS and kept at 25°C. Cells were transfected with 2 μg plasmid DNA using FuGENE® HD Transfection Reagent. RNAi treatment and dsRNA synthesis was performed as previously described (21). The knockdown efficiency was further confirmed by western blot.

ChIP-Seq assay

Chromatin immunoprecipitation was carried out as previously described (22). Briefly, 10^7 cells were used for each IP. Cells were cross-linked in 1% formaldehyde at room temperature for 10 min then the formaldehyde was quenched by addition of Glycine to a final concentration of 125 mM. Nuclei were isolated by adding 1 ml ice-cold IP buffer (150 mM NaCl, 50 mM Tris–HCl (pH 7.5), 5 mM EDTA, NP-40 (0.5%, vol/vol), Triton X-100 (1.0% vol/vol)) supplemented with EDTA-free protease inhibitor cocktail (Roche) and 5 μl/ml PMSF (100 mM). Nuclei were washed in IP buffer then resuspended in 1ml IP buffer. Nuclei were sonicated using bioruptor for 15 cycles (30 s on and 30 s off). Cleared chromatin was incubated with the antibodies overnight at 4°C on rotating wheel. Aliquot 40 μl protein A/G slurry were added to each IP. After 1 h, the beads were washed five times and the DNA was extracted using Chelex-100 resin (Bio-Rad). Sequencing libraries were prepared from 10 ng of immunoprecipitated DNA with the Illumina ChIP-Seq DNA Sample Prep Kit according to Illumina's instructions. Cluster generation was performed using the Illumina cluster station, sequencing on the HiSeq 2500 followed a standard protocol. The fluorescent images were processed to sequences using the Genome Analyzer Pipeline Analysis software 1.8 (Illumina). The reads were then mapped to dm3 with Bowtie (23) and peaks were called using MACS1.4 (24), while differential peak binding was calculated using two alternative strategies. On the one hand HOMER software (25) was used with the command getDifferentialPeaks (default settings with $\log_2$ fold reduction set to –F 2). This approach uses read count normalization based on total number of reads per library and is summarized in Figure 2B. In an independent approach extraction of read counts per Gcn5 peak was done using BioConductor packages (26) GenomicRanges (27) and Rsamtools (http://bioconductor.org/packages/release/bioc/html/Rsamtools.html) (28). We calculated the union of Gcn5 peaks called in independent experiments and extracted corresponding read counts. Normalization of the resulting count matrix and identification of differentially bound peaks and corresponding confidence intervals was done using DESeq2 with default settings (29) (Figure 2C and D). Heat maps and average plots were generated using seqMINER (30) and NGSplot (31), using default settings, respectively. All other plots were generated using R (http://www.R-project.org) (32). Genome browsers snapshots were generated using Gviz Biocondutor package (33).

Co-immunoprecipitation and mass spectrometry

Wildtype S2 cells (120×10^6 cells) were harvested. Nuclei were isolated and the immunoprecipitation was carried out as previously described (34). The immunoprecipitated proteins were separated on SDS-PAGE (4–12%) then the peptides were extracted using In-Gel trypsinization method as previously described (35). The amount of peptides was measured using label-free quantification method (LFQ), and then the ratio between Gcn5 IP/IgG was calculated.

RNA-Seq

RNA extraction was carried out using TRIzol extraction method. For each experimental condition we prepared two biological replicates from 1 μg total RNA. RNA was depleted of rRNA using Ribo-Minus technology. Libraries were prepeared from purified RNA using ScriptSeq™ v2 and were sequenced on an Illumina HiSeq 2500. Read mapping was done with Bowtie2 called from TopHat (36) with default settings. For known transcript models we used dm3 RefSeq (UCSC) annotations downloaded from Illumina's iGenome repository. The aligned reads were analysed with custom R scripts in order to obtain gene expression measures. For normalization of read counts and identification of differentially expressed genes we used DESeq2 (29) with default settings. Overlap between gene lists obtained from different treatments was analysed by the GeneOverlap BioConductor package (http://shenlab-sinai.github.io/shenlab-sinai/) (37).

Antibodies

Rabbit polyclonal anti-dCTCF (15): for each IP 5 μl were used. Mouse monoclonal anti-CP190 (gift from Harald

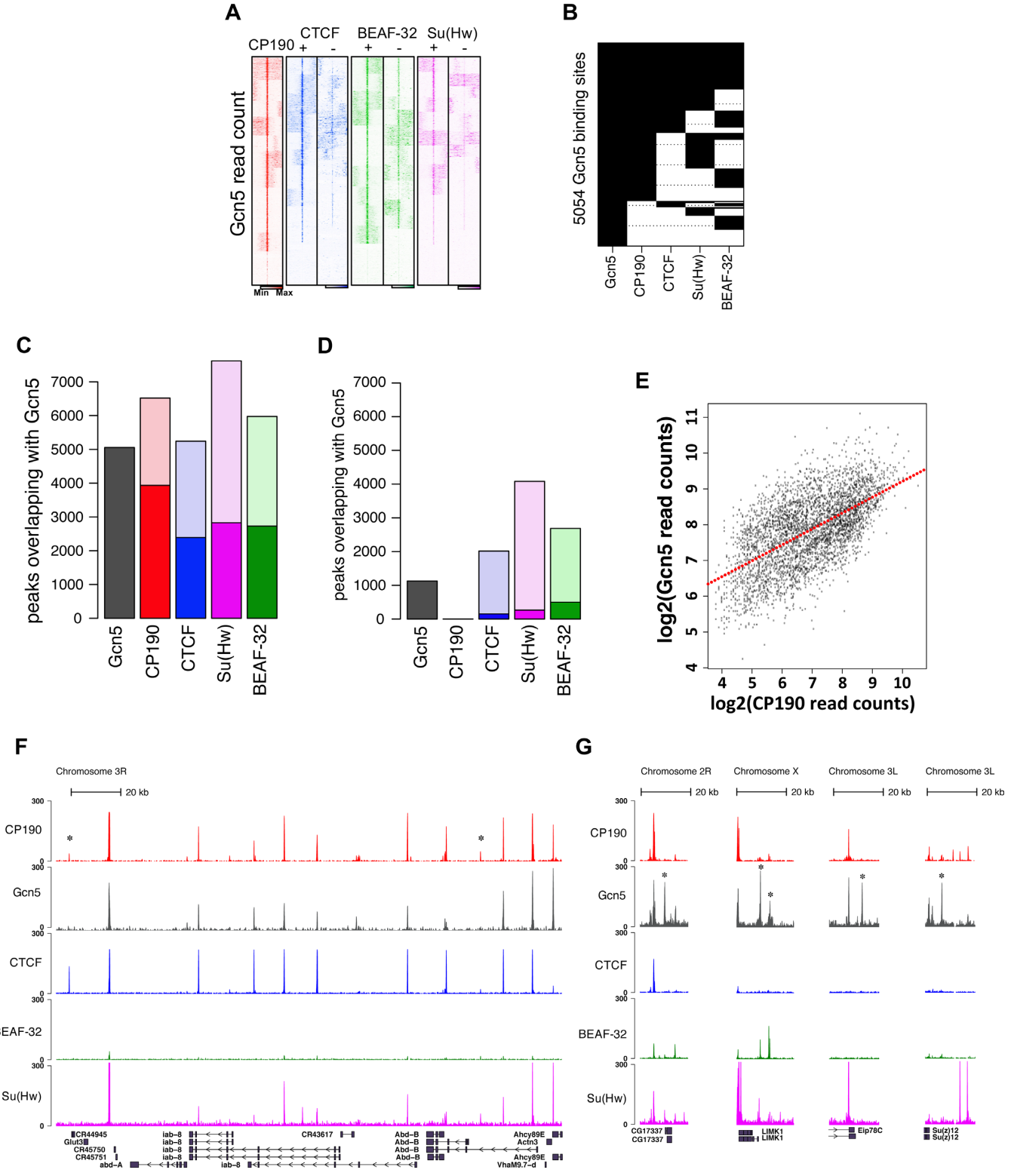

Figure 1. Gcn5 ChIP-Seq. (**A**) Density heatmaps of Gcn5 reads over insulator binding proteins in Kc cells. K-means clustering of normalized Gcn5-specific reads with CP190 (red) sites, dCTCF (blue) sites that overlap with CP190 (+) and those that don't overlap with CP190 (–), BEAF-32 (green) and Su(Hw) (purple) sites (±3 kb). (**B**) Binary heat map (black = overlapping binding) indicates overlap of 5054 Gcn5 binding sites detected in Kc cells with several insulator factors (publicly available data from GEO: GSM762842, GSM762836, GSM762839 and GSM762845). (**C**) Barplot shows total numbers of binding sites for the analysed factors, where dark colours indicate the fraction of sites overlapping with Gcn5. The highest fraction of sites overlapping with Gcn5 shows CP190. (**D**) Barplot as in (C), but only binding sites devoid of CP190 are depicted. Only minor fractions of insulator sites devoid of CP190 are overlapping with Gcn5. (**E**) Scatter plots with linear regression between Gcn5 and CP190 read counts. The correlation shows a strong correlation coefficient (0.6). (**F**) Genome-browser snapshots of Gcn5 and CP190 binding. Gcn5 and CP190 ChIP-Seq profiles at BX-C (200 kb) showing co-occurrence at the insulator regions between segment-specific homeotic genes. (**G**) Gcn5 standalone peaks (*) that do not overlap with CP190 and/or with other insulator factors (CG17337, LIMK1, Eip78C and Su(z)12).

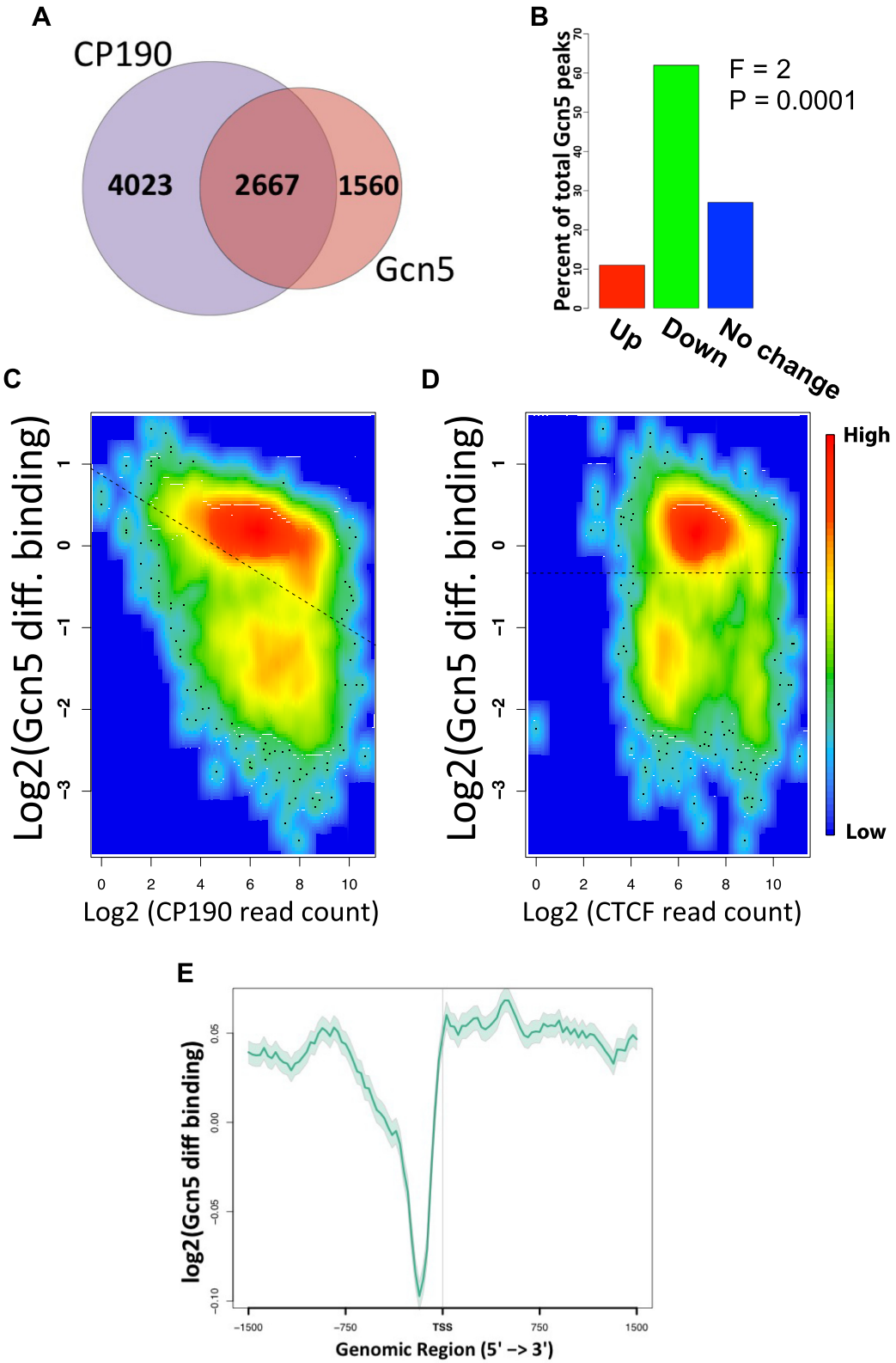

Figure 2. Gcn5 ChIP-Seq analysis in Kc cells after CP190 depletion: (**A**) Venn diagram showing Gcn5 peaks that overlap with CP190 after CP190 kd. (**B**) Differential Gcn5 peaks which still overlap with CP190 after CP190 kd. 62% of the 2667 Gcn5 peaks with a Poisson *P*-value < 0.0001 underwent at least a two-fold reduction after CP190 kd ($F = 2$) (green). (**C** and **D**) Binding dependency of Gcn5 on CP190, but not on CTCF. 2D density representation of scatterplots show differential Gcn5 binding as a function of CP190 (C) or CTCF (D) read counts across all Gcn5 peaks. Scale bar in (D) indicates colour coding of densities. Linear models were fitted (dotted lines) and indicate a negative linear relationship between CP190 binding and differential Gcn5 binding (C, $P < 2.2e{-}16$), which is not the case for CTCF (D, $P = 0.967$). (**E**) Average profile of Gcn5 loss across genomic regions revealing that many of the Gcn5 reduced peaks after CP190 depletion are in the promoter region. The semi-transparent grey shade around the average signal indicates the interval of the average change of signal ± the standard error of the mean.

Saumweber): 20 μl were used for each IP, whereas a dilution of 1:2500 was used for western blot. Rabbit polyclonal anti-Gcn5 (gift from Aleksey Krasnov): 5 μl were used per IP and 1:5000 for western blot. Rabbit anti-H3 (Abcam, ab1791): 5 μl were used for each IP. Mouse monoclonal anti-Flag (M2, Sigma F3165): 10 μl were used for each IP. Mouse anti-beta tubulin (DSHB Hybridoma Product E7): a dilution of 1:25000 was used in western blot and Rabbit anti-H3K27me3 (Abcam, # ab6002): 5 μl were used for each IP.

Primers

See Supplementary Table S3.

RESULTS

Gcn5 binding is strongly correlated with CP190 binding

In order to generate a high-resolution genome-wide Gcn5 binding map, affinity-purified Gcn5 polyclonal antibody was used for ChIP-Seq analysis of *Drosophila* Kc cells. The specificity of the Gcn5 antibody was determined according to the modENCODE guidelines. qPCR of precipitated chromatin from Gcn5 depleted cells, using two different dsRNA sequences, resulted in reduced ChIP and western signals and loss of the H3K9ac mark (Supplementary Figures S1 and S2B). Gcn5 ChIP-Seq reads were clustered over CP190 peaks (GSM762836) using the *K*-means clustering method. Gcn5 reads are strongly enriched over CP190 peaks (Figure 1A). We determined 5095 Gcn5 peaks and compared these with the previously identified 6690 CP190 peaks. 60% of all CP190 peaks overlap with 78% of all Gcn5 peaks (Figure 1B-D). As CP190 is known to bind to promoters as well as to all DNA-binding insulator factors (1), we compared the distribution of Gcn5 reads with those of three insulator factors dCTCF (GSM762842), BEAF-32 (GSM762845) and Su(Hw) (GSM762839). Again, high Gcn5 read densities are detected at insulator-bound sites, especially when these are co-bound by CP190 (Figure 1A). Overlap-analysis of these five factors again revealed the strongest overlap between CP190 and Gcn5 (Figure 1B). Pairwise comparison of Gcn5 with the other factors showed a substantial overlap between all pairs, with the highest overlap fraction in case of Gcn5 and CP190 (Figure 1C). As a control, the insulator sites devoid of CP190 binding were separately analysed. These showed a marginal overlap with Gcn5 (Figure 1D). Thus, Gcn5 binding to insulator sites is correlated with the presence of CP190. To further characterize the overlap between CP190 and Gcn5, we compared the binding strength of both factors at overlapping sites (Figure 1E). There is an obvious correlation (correlation coefficient of 0.6) in binding strength of both factors, suggesting that there may be interdependence between them. In order to visualize this strong overlap, a genome browser snapshot of the bithorax complex is presented (Figure 1F). CP190 peaks (red) are mostly overlapping with Gcn5 peaks (grey) in addition to the presence of two CP190-standalone peaks devoid of Gcn5 (asterisks). Additional genomic regions are shown (Figure 1G) to demonstrate Gcn5-standalone sites as well.

CP190 recruits Gcn5 to chromatin at CP190 binding sites

Based on the correlation of CP190 and Gcn5 sites we wanted to determine, whether CP190 may be a recruiter for Gcn5. Therefore, we depleted CP190 in Kc cells by dsRNA (Supplementary Figure S2A) and tested for genome-wide binding of Gcn5 by ChIP-Seq. The number of 5095 Gcn5 peaks after control knockdown (dsRNA against GFP) was reduced to 4227 peaks after CP190 knockdown. However, 2667 Gcn5 peaks remained at CP190 sites (Figure 2A). To identify any change in binding strength of the remaining Gcn5 sites after CP190 depletion, we applied differential binding analysis on these 2667 peaks. We found that 62% of the peaks underwent a reduction of at least two-fold (Figure 2B), while 11% increased and 27% remained unchanged. Furthermore, depletion of CP190 from strong binding sites should cause stronger binding changes of Gcn5 as compared to weak CP190 sites. This is indeed the case (Figure 2C). A significant correlation between Gcn5 binding changes upon CP190 depletion and CP190 binding strength is detected. In contrast, when analysing the Gcn5 binding changes with respect to dCTCF binding strength, there is no correlation detected (Figure 2D). ChIP-qPCR of CP190 binding sites grouped in respect to binding strength showed a similar result with a strong dependency of Gcn5 binding on CP190 at strong CP190 binding sites (Supplementary Figure S3). Thus, we can conclude that CP190 recruits Gcn5 to CP190 bound sites. To test for a preferential location of CP190 dependent Gcn5 binding we determined the average profile of Gcn5 binding changes across the genome (Figure 2E). A specific location is the region just upstream of the TSS. In this region Gcn5 binding is highly dependent on CP190.

In order to validate the ChIP-Seq results, the CP190 RNAi experiment was carried out in three biological replicates and ChIP-qPCR reactions were performed (Figure 3). From the ChIP-Seq results we chose twenty sites, representing four different groups, sites positive for dCTCF, CP190 and Gcn5, sites positive for CP190 and Gcn5, Gcn5-standalone sites and sites negative for any of these three factors. As a knockdown control we used GFP-dsRNA (GFP kd) and for specific knockdown we used a double knockdown (dkd) against CP190 and against dCTCF (CP190/CTCF dkd) to achieve a better depletion of CP190 at dCTCF binding sites. For unspecific precipitation we used IgG. Negative sites and the IgG precipitation show a background PCR signal only. All dCTCF/CP190 and all CP190 sites show the expected specific signals, which are markedly reduced after CP190/CTCF dkd. Furthermore, the CP190/CTCF dkd causes a strong reduction in Gcn5 precipitation at sites positive for CP190 irrespective of the presence of dCTCF. Thus, the knockdown effect can be attributed to CP190 depletion. Gcn5-standalone sites remain unchanged (Figure 3). The reverse experiment to deplete Gcn5 and determine CP190 binding was done as well (Supplementary Figure S3). The binding of CP190 is only slightly effected by Gcn5 depletion, whereas the binding of Gcn5 is highly dependent on CP190.

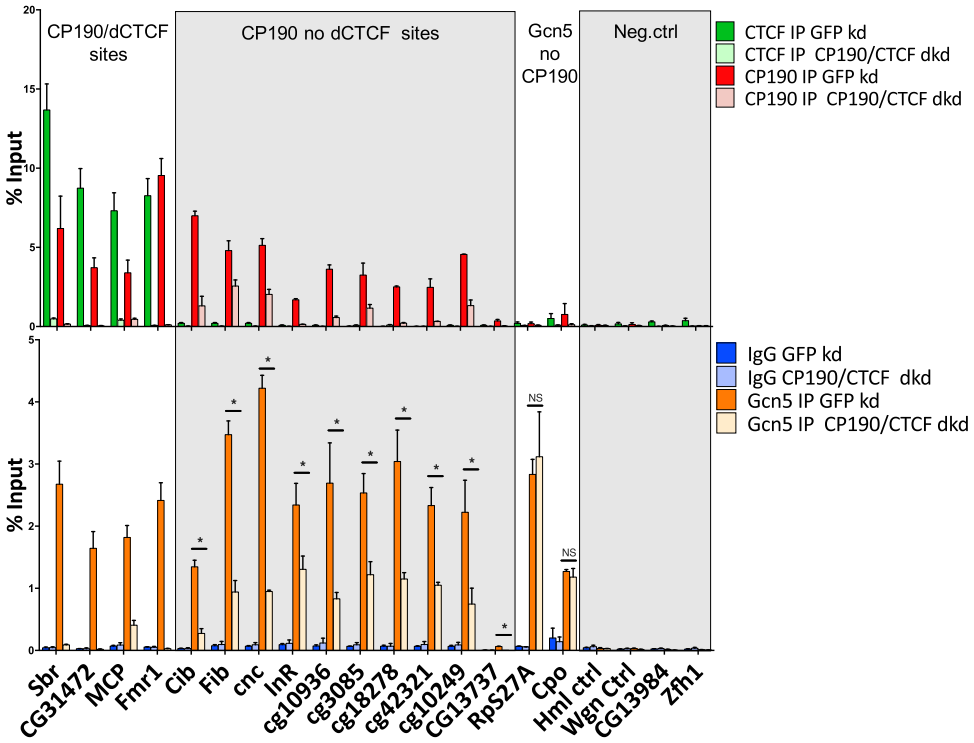

Figure 3. Gcn5 binding is dependent on CP190 at CP190 sites. Upper panel: CP190 and CTCF ChIP after Kc cells treatment with dsRNA against CP190 and CTCF (CP190/CTCF dkd). qPCRs showing reduction of CTCF and CP190 at their respective sites in comparison to GFP knockdown. Lower panel: Gcn5 ChIP-after CP190/CTCF depletion shows Gcn5 reduction at all CP190 sites. Gcn5 binding at sites devoid of CP190 binding (RpS27A and Cpo) remain unchanged. The data represented as $M \pm$ SD using three biological replicates. Asterisk represent significance level <0.01 after paired *t*-test, NS indicates no significant difference.

Gcn5 is physically interacting with CP190

Endogenous Gcn5 was immunoprecipitated from embryonic S2 cells in two independent biological replicates. The immunocomplex was separated on gradient SDS-PAGE and peptides were extracted after in-gel trypsinization. Mass-spectrometry identified, as expected, most of the SAGA and ATAC complex components (Supplementary Table S1) Atac1, Atac2, Ada2b, Sgf29, Taf module subunits (Taf4, Taf5, Taf6 and Saf6) and Spt module subunits (Spt1, Spt3, Spt4, Spt5 and Spt20). For both complexes Gcn5 is the central component (38). In addition to these, CP190 was found and ranked within the highest top mascot scores in both biological replicates under stringent washing conditions (Figure 4A). Furthermore, factors known to interact with CP190 were found, such as Dref. This factor, similarly to CP190, is found at active promoters and at insulators (21,39,40). The factors Pzg and Chro, both of which are associated with the NURF complex and are colocalized genome-wide with CP190 (21,41), are detected in the Gcn5 immunocomplex (Figure 4A). In order to further confirm the Gcn5/CP190 interaction, we carried out immunoprecipitations of Gcn5. The precipitate was clearly positive for CP190 (Figure 4B).

Overlapping function of Gcn5 and CP190

Based on the striking overlap of Gcn5 and CP190 binding sites we predicted that an overlapping set of genes should be affected upon depletion of either factor. Depletion of CP190 deregulated 383 genes, when compared to the unspecific GFP knockdown. This number is in the range reported in other publications (42,43). These included 152 up-regulated and 231 down-regulated genes. Gcn5 depletion deregulates 1100 genes (468 up-regulated genes and 632 down-regulated genes) when compared to GFP kd (similar numbers were reported by (44)).

If CP190 is the recruiter for Gcn5, one would predict a significant number of genes being co-regulated. Therefore, we sorted the genes according to the $\log_2$ fold expression change after CP190 kd into genes up-regulated or down-regulated (Figure 5A). In most cases, the expression change after Gcn5 kd follows the change seen after CP190 depletion. In focusing on genes showing an expression change with an adjusted *P*-value of 0.05 or less, we find 52% of the CP190 deregulated genes to be deregulated by Gcn5 depletion as well (Figure 5B). As tested by qPCR, the knockdown of CP190 and Gcn5 resulted in significant reduction of the respective factor, whereas CP190 seemed to be up-regulated after Gcn5 kd (Figure 5C). On the protein level, this up-regulation was only marginal (Supplementary Figure S2B). In order to verify the finding of CP190 and Gcn5 co-regulated genes, we applied more stringent filtering parameters (*P*-value of 0.05 and $\log_2$ fold change of 0.7), resulting in a lower number of deregulated genes (Supplementary Figure S4). Yet, again, genes deregulated by either factor are significantly overlapping (Supplementary Figures S4 and S5). Furthermore, these deregulated genes show a

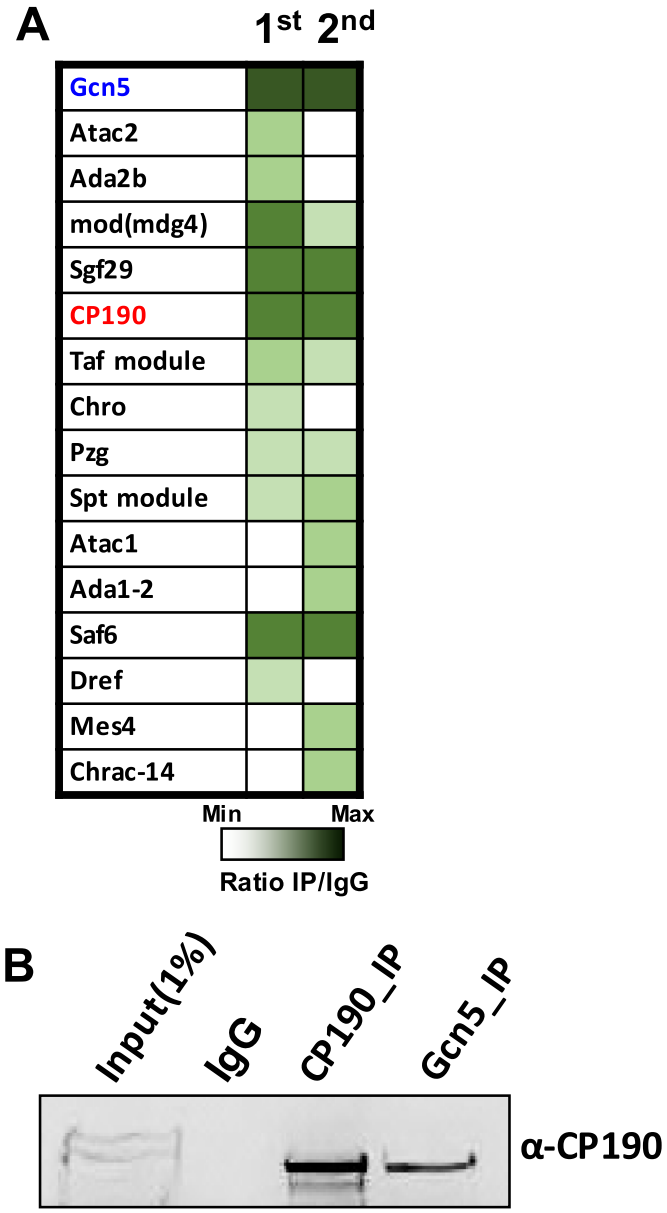

Figure 4. Gcn5 immunoprecipitation from S2 cells. (**A**) Mass spectrometry top hits in two biological replicates reveal that CP190 as well as most of SAGA subunits are co-eluted with Gcn5. (**B**) Co-IP validates the interaction between Gcn5 and CP190.

significant positive correlation (*P*-value = 2.6e–6) (Supplementary Figure S6).

In summary, we can conclude that a co-regulation of a significant number of genes is found with a majority of these being activated by the presence of both factors. This suggests a model involving DNA binding factors like IBPs, binding CP190, which in turn recruits Gcn5. Such an arrangement would be predicted to cause gene activation based on the activation function of Gcn5. As a crucial test for such a function we wanted to target either CP190 or Gcn5 to a silent gene locus to test the effect of either factor on this locus. We chose the even-skipped (*eve*) gene, which is expressed in the first 6 hours after fertilization. In the late embryonic stage, polycomb proteins shut down *eve* gene expression completely (13). In Kc as well as in S2 cells, the *eve* gene is embedded in an H3K27me3 domain and insulated from the surrounding highly expressed genes by Homie/NHomie insulators (Figure 6B) (13,45–47). For specific targeting we used the CRISPR/Cas9 system with a catalytically inactive protein dCas9 (48). We generated fusion constructs of Flag-dCas9 with Gcn5 or with CP190 (Figure 6A). In addition, this construct expresses a guide RNA specific for the *eve* locus, which is required to target the dCas9 fusion proteins to this locus. We generated two S2 cell clones for each of the fusion constructs and found both of them similarly expressed (Supplementary Figure S2C). Although these fusion proteins are quite large, proteins of the expected full-length molecular weight were detected. As a negative control we also generated cell clones expressing the original dCas9 vector with the same *eve*-specific guide RNA, but without a Gcn5 or CP190 fusion. The binding of dCas9 in the negative control clone (dCas9) and in two selected clones (dCas9CP190 clone 2 and dCas9Gcn5 clone 6) to the site of the target sequence was confirmed by FLAG ChIP-qPCR using primers flanking the guide RNA sequence (green arrow in Figure 6B) and primers for a negative site about 3 kb downstream within the same domain (yellow arrow Figure 6B). The binding of dCas9 was clearly detected at the target site when compared to the negative control site (Figure 6C). Since the *eve* gene is embedded within a facultative H3K27me3 domain (Figure 6B), we wanted to know whether this modification may have been changed in case of expression and targeting of either dCas9 fusion proteins. Indeed, when we carry out chromatin IP with an antibody against H3K27me3, we find that the two cell clones C2 and C6 show reduced H3K27me3 levels at the integration site, when compared to the dCas9 control cell clone. In contrast, the downstream control site is not changed in the level of H3K27me3 (Figure 6D, Supplementary Figure S7). When testing *eve* expression in the negative control clone and in both of the dCas9 fusion clones, for each of the fusions we found that both clones expressing either dCas9 fusion induced *eve* expression (Figure 6E).

This result confirms that both CP190 and Gcn5 are similarly acting as transcriptional activators.

DISCUSSION

Drosophila insulator binding proteins (IBPs) are characterized by a multitude of different factors, with only one of which, CTCF, being highly conserved from insects to mammals. CP190, not found in vertebrates, seems to be the unifying factor associated with all of the known *Drosophila* IBPs. Analysis of genome-wide binding revealed clusters of IBPs bound to CP190. Therefore, it is not surprising to find CP190 enriched at chromatin-domain boundaries (14). In addition, CP190 has been found at promoters of active genes (15). Both features, binding to promoters and to domain boundaries, require some kind of bridging, either with enhancers or between paired domain boundaries. In fact, CP190 has been demonstrated to contact and bridge several IBPs (3,49,50). In addition to looping and bridging, CP190 has been implicated in modifying chro-

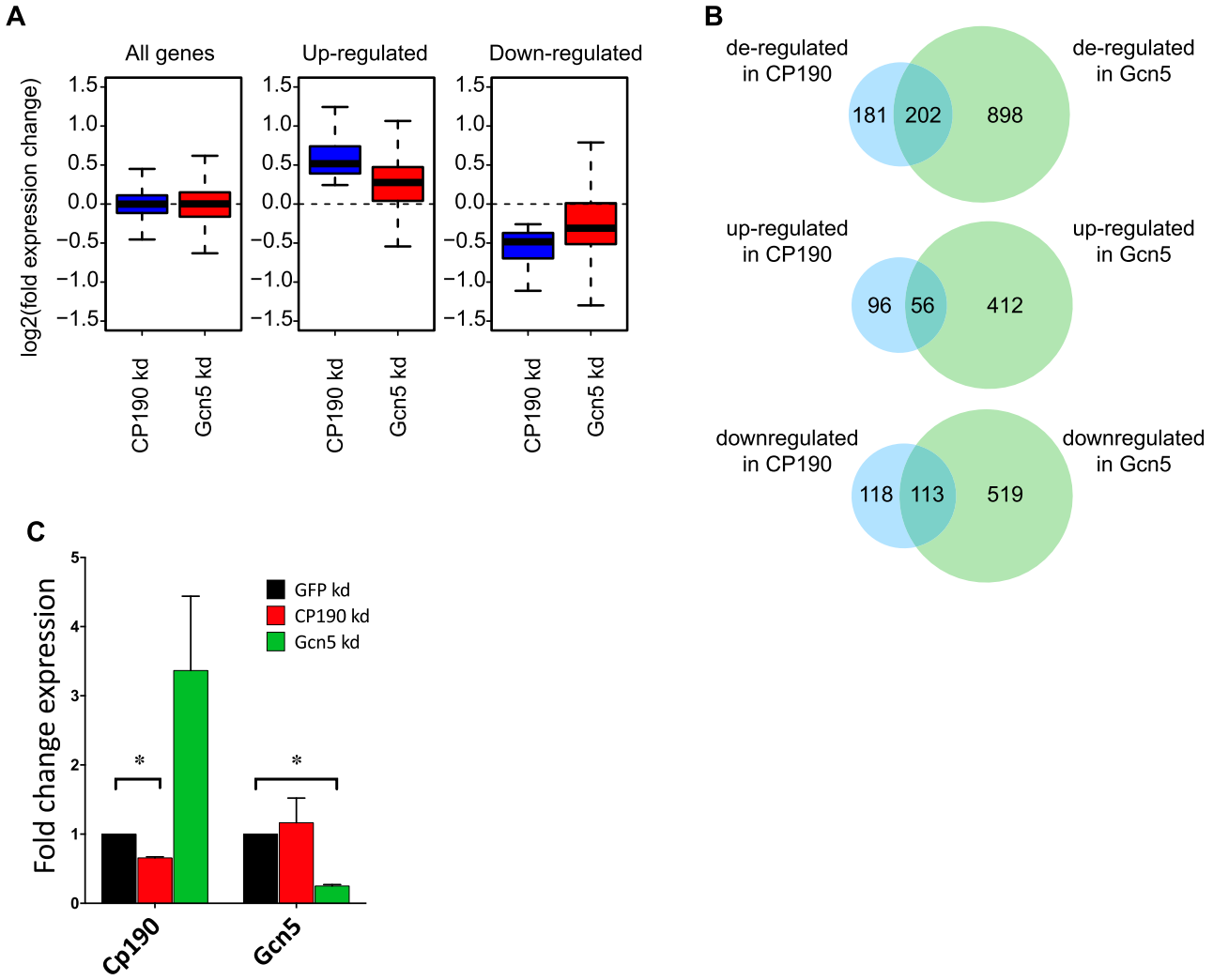

Figure 5. RNA-Seq in S2 cells. (**A**) Boxplot of $\log_2$ fold change after CP190 kd (blue) and Gcn5 depletion with dsRNA specific for two different Gcn5 sequences (red) shown for all genes (left), genes that are significantly up-regulated after CP190 depletion (center) and genes that are significantly down-regulated (adjusted $P < 0.05$) after CP190 depletion (right). Within the class of up-regulated genes the $\log_2$ fold change after Gcn5 depletion is significantly higher than for the average gene (Wilcoxon signed rank test: $P < 2.2e{-}16$). Conversely, within the class of down-regulated genes the $\log_2$ fold change after Gcn5 depletion is lower than average ($P < 2.2e{-}16$). (**B**) Venn diagrams showing significant overlap between significantly (adjusted $P < 0.05$) de-regulated, down-regulated and up-regulated genes in CP190 and Gcn5 RNAi relative to GFP. In all cases, the observed overlap was significant (hypergeometric $P < 2.2e{-}16$, odds ratios were for generally de-regulated, down-regulated and up-regulated genes 7.72, 12.43 and 9.8, respectively). In contrast there was no such strong association between conversely regulated genes (Supplementary Figure S4B). (**C**) CP190 and Gcn5 RNA levels as determined by rt-PCR after knockdown of CP190 (green) and of Gcn5 (red). The data are represented as $M \pm$ SD using two biological replicates. Significance (unpaired t-test) is indicated (*).

matin. dCTCF/CP190 binding sites show reduced nucleosomal occupancy, whereas dCTCF sites devoid or depleted of CP190 are loaded with nucleosomes (15). Furthermore, CP190 binding sites have been found to be enriched for active histone marks (16). Therefore, we searched for a factor potentially involved in modifying chromatin and being co-localized with chromatin bound by CP190.

Here, we find CP190 chromatin binding to be strongly correlated with Gcn5 genome-wide. Gcn5 is a highly conserved acetyltransferase, which is a component of the SAGA chromatin-modifying complex (for reviews see (38,51)). Deficiencies of SAGA components cause severe developmental defects, suggesting that SAGA and Gcn5 contribute to the transcriptional regulation of developmental genes.

The correlation between Gcn5 and CP190 binding is found for 75% of the Gcn5 sites and for 60% of the CP190 sites. The overlap between CP190 and Gcn5 is stronger than that between Gcn5 and Su(Hw), dCTCF and BEAF-32 standalone sites (Figure 1). Moreover, Gcn5 co-occurs with CP190 at CP190 standalone sites (Figure 3). Previously, the occurrence of SAGA components ENY2, Ada2b or of Gcn5 has been detected at selected dCTCF or Su(Hw) sites (20,52,53), which now may be explained in part due to CP190 binding at these sites in addition to direct contacts with dCTCF or Su(Hw).

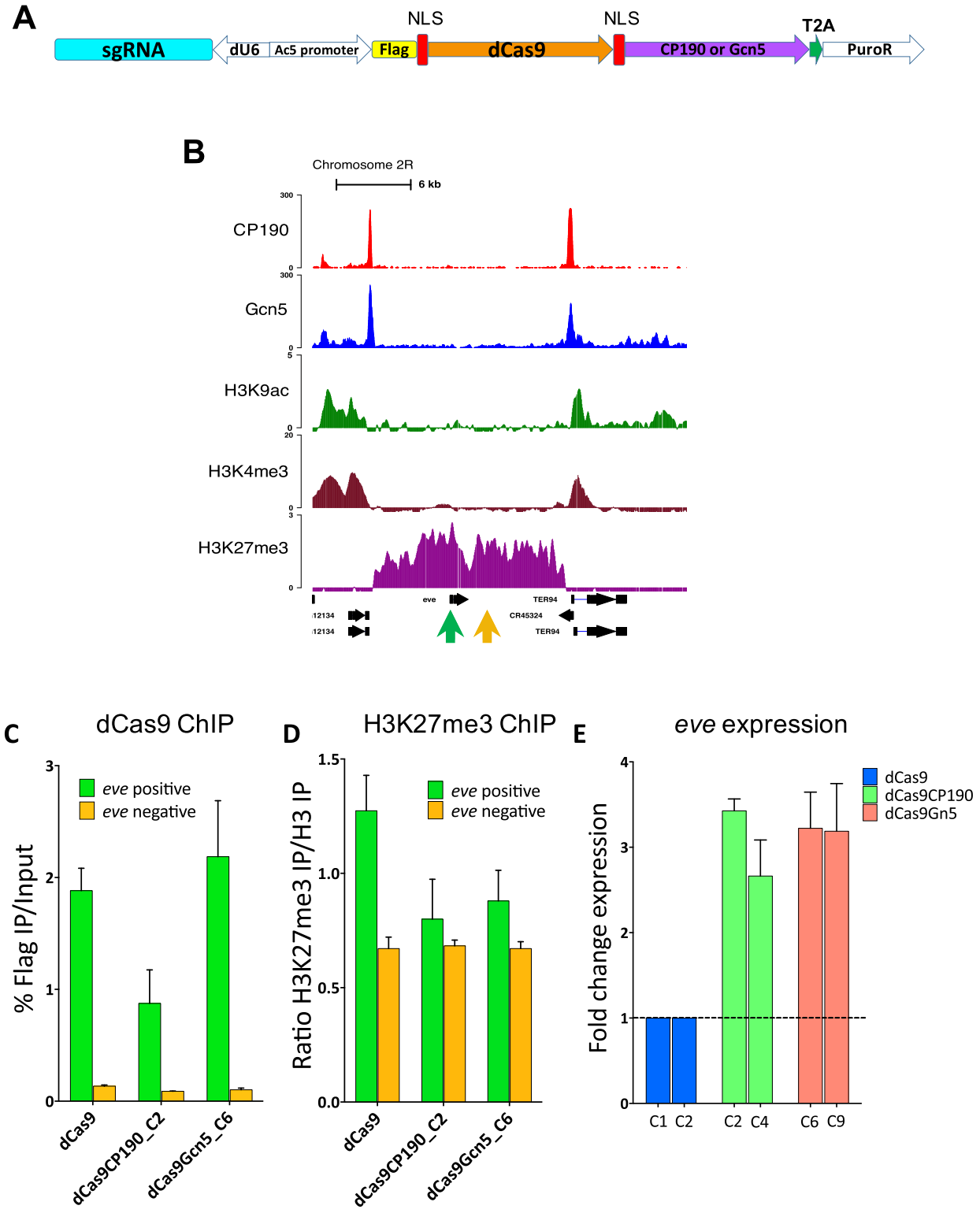

Figure 6. Cas9-directed binding of CP190 or of Gcn5 activates the H3K27me3 repressed *eve* locus. (**A**) dCas9 fusions targeting *eve* locus. The dCas9 vector codes for the sgRNA scaffold and for dCas9 fused to CP190 or to Gcn5. (**B**) The genome browser snapshot of the *eve* locus indicates the dCas9 crRNA target sequence (green arrow). A non-targeting site is pointed out (yellow arrow), which was used as negative control. (**C**) Flag ChIP-qPCR validates the specific binding of dCas9 or of dCas9 fusions at the *eve*-locus crRNA target site (green bars) compared to a non-targeting negative site (yellow bars). (**D**) H3K27me3 ChIP at dCas9 positive and negative sites normalized to H3 levels. Both, dCas9CP190 and dCas9Gcn5 reduce H3K27me3 at the binding site (green bars) in contrast to the non-targeting site (yellow bars). (**E**) The normalized expression of the *eve* gene in dCas9, dCas9CP190 and dCas9Gcn5 expressing S2 cell clones. For each construct two clones are shown. The recruitment of CP190 and Gcn5 increases *eve* gene expression significantly. The data are represented as M±SD using two biological replicates.

The data presented here suggest that Gcn5 and CP190 binding not only show a strong correlation, but rather that Gcn5 chromatin binding is even dependent on CP190. This is further supported by the co-purification of Gcn5 and of CP190. In addition to binding of Gcn5 to CP190, the SAGA component ENY2 has been shown to interact with the zinc finger domains of Su(Hw) and of dCTCF (52,53).

Despite the fact that depletion of Gcn5, or of other SAGA components or of CP190 affects a limited number of genes (13,15,44), we were able to detect a significant overlap of genes with changed expression after depletion of Gcn5 and of CP190. In fact, the number of genes being impaired by either depletion is higher as compared with the genes being activated. This suggests, that both, CP190 and Gcn5, in many cases function as activators. This confirms previous data showing the co-activator function of Gcn5 or of CP190 (13,15,44,54).

Several mechanisms of Gcn5 action have been reported. One of the aspects is the connection to DNA replication and cell cycle. The insulator protein Su(Hw) has been shown to recruit Gcn5 to the origin recognition complex (ORC) (20). Furthermore, binding sites for *Drosophila* IBPs, especially dCTCF and CP190, correlate strongly with replication origins that are enriched at gene promoters (55,56). Interestingly, CP190 recruits Dref (replication-related element-binding factor), which regulates cell cycle progression and replication (40).

Dref is also found to bind to CP190 and to be required for the Fab8 insulator to mediate enhancer-blocking (21). Another acetyltransferase, Myst5, has been shown to colocalize with Dref and the factors Chro (chromator) and Pzg (Putzig) together with other insulator proteins at active gene promoters (41). Here, we show that all three factors purify with Gcn5 and all have been isolated with CP190 (21). This suggests that acetyltransferases, such as Gcn5 or Myst5 may play a functional role in insulation. In fact, the SAGA component ENY2 is recruited to the zinc-finger domain of dCTCF and is required for the barrier activity of dCTCF and of Su(Hw)-dependent insulators (52,53). Furthermore, the NURF complex and Gcn5 have been shown to functionally interact (44). Again, the connection to insulator function has been demonstrated by purifying NURF components with CP190 and showing the requirement for NURF in enhancer blocking (21).

The acetylation activity of Gcn5 has been shown with multiple lysines within histone H3 as substrate. Depletion of Gcn5 results in a reduction of acetylation of lysines 9, 14 and 27 (57) indicating the overall activation function of Gcn5, which we confirm as well by the higher number of repressed genes after Gcn5 depletion. In general, histone acetylation is connected to chromatin opening. It has been shown that depletion of histone acetyltransferases increases nucleosome occupancy as Gcn5 relaxes chromatin and increases chromatin openness (58,59). Gcn5 mediated nucleosome eviction has been demonstrated (60). Such a function may contribute to the finding that CP190 binding sites are depleted from nucleosomes (15,21,61,62).

In summary, for all of the factors involved and recruited by CP190, such as NURF (21,62), DREF (62,63) and Gcn5 (60), nucleosome depletion has been demonstrated. Here, the concerted action of CP190 recruiting these factors may result in efficient nucleosome removal.

SUPPLEMENTARY DATA

Supplementary Data are available at NAR Online.

ACKNOWLEDGEMENTS

We are grateful to Aleksey Krasnov for the generous gift of the Gcn5 antibody and Harald Saumweber for the CP190 antibody. We would like to thank Leni Schäfer-Pfeiffer for excellent technical assistance.

FUNDING

Deutsche Forschungsgemeinschaft [TRR81]; DAAD. Funding for open access charge: DFG TRR81.
Conflict of interest statement. None declared.

REFERENCES

1. Ali,T., Renkawitz,R. and Bartkuhn,M. (2016) Insulators and domains of gene expression. *Curr. Opin. Genet. Dev.*, **37**, 17–26.
2. Cuartero,S., Fresan,U., Reina,O., Planet,E. and Espinas,M.L. (2014) Ibf1 and Ibf2 are novel CP190-interacting proteins required for insulator function. *EMBO J.*, **33**, 637–647.
3. Maksimenko,O., Bartkuhn,M., Stakhov,V., Herold,M., Zolotarev,N., Jox,T., Buxa,M.K., Kirsch,R., Bonchuk,A., Fedotova,A. *et al.* (2015) Two new insulator proteins, Pita and ZIPIC, target CP190 to chromatin. *Genome Res.*, **25**, 89–99.
4. Zhao,K., Hart,C.M. and Laemmli,U.K. (1995) Visualization of chromosomal domains with boundary element-associated factor BEAF-32. *Cell*, **81**, 879–889.
5. Geyer,P.K. and Corces,V.G. (1992) DNA position-specific repression of transcription by a Drosophila zinc finger protein. *Genes Dev.*, **6**, 1865–1873.
6. Holdridge,C. and Dorsett,D. (1991) Repression of hsp70 heat shock gene transcription by the suppressor of hairy-wing protein of Drosophila melanogaster. *Mol. Cell. Biol.*, **11**, 1894–1900.
7. Gaszner,M., Vazquez,J. and Schedl,P. (1999) The Zw5 protein, a component of the scs chromatin domain boundary, is able to block enhancer-promoter interaction. *Genes Dev.*, **13**, 2098–2107.
8. Gerasimova,T.I., Lei,E.P., Bushey,A.M. and Corces,V.G. (2007) Coordinated control of dCTCF and gypsy chromatin insulators in Drosophila. *Mol. Cell*, **28**, 761–772.
9. Mohan,M., Bartkuhn,M., Herold,M., Philippen,A., Heinl,N., Bardenhagen,I., Leers,J., White,R.A., Renkawitz-Pohl,R., Saumweber,H. *et al.* (2007) The Drosophila insulator proteins CTCF and CP190 link enhancer blocking to body patterning. *EMBO J.*, **26**, 4203–4214.
10. Moon,H., Filippova,G., Loukinov,D., Pugacheva,E., Chen,Q., Smith,S.T., Munhall,A., Grewe,B., Bartkuhn,M., Arnold,R. *et al.* (2005) CTCF is conserved from Drosophila to humans and confers enhancer blocking of the Fab-8 insulator. *EMBO Rep.*, **6**, 165–170.
11. Holohan,E.E., Kwong,C., Adryan,B., Bartkuhn,M., Herold,M., Renkawitz,R., Russell,S. and White,R. (2007) CTCF genomic binding sites in Drosophila and the organisation of the bithorax complex. *PLoS Genet.*, **3**, e112.
12. Ohtsuki,S. and Levine,M. (1998) GAGA mediates the enhancer blocking activity of the eve promoter in the Drosophila embryo. *Genes Dev.*, **12**, 3325–3330.
13. Van Bortle,K., Ramos,E., Takenaka,N., Yang,J., Wahi,J.E. and Corces,V.G. (2012) Drosophila CTCF tandemly aligns with other insulator proteins at the borders of H3K27me3 domains. *Genome Res.*, **22**, 2176–2187.
14. Van Bortle,K., Nichols,M., Li,L., Ong,C., Takenaka,N., Qin,Z. and Corces,V. (2014) Insulator function and topological domain border strength scale with architectural protein occupancy. *Genome Biol.*, **15**, R82.

15. Bartkuhn,M., Straub,T., Herold,M., Herrmann,M., Rathke,C., Saumweber,H., Gilfillan,G.D., Becker,P.B. and Renkawitz,R. (2009) Active promoters and insulators are marked by the centrosomal protein 190. *EMBO J.*, **28**, 877–888.
16. Ulianov,S.V., Khrameeva,E.E., Gavrilov,A.A., Flyamer,I.M., Kos,P., Mikhaleva,E.A., Penin,A.A., Logacheva,M.D., Imakaev,M.V., Chertovich,A. *et al.* (2016) Active chromatin and transcription play a key role in chromosome partitioning into topologically associating domains. *Genome Res.*, **26**, 70–84.
17. Ringel,A.E., Cieniewicz,A.M., Taverna,S.D. and Wolberger,C. (2015) Nucleosome competition reveals processive acetylation by the SAGA HAT module. *Proc. Natl. Acad. Sci. U.S.A.*, **112**, E5461–E5470.
18. Krebs,A.R., Karmodiya,K., Lindahl-Allen,M., Struhl,K. and Tora,L. (2011) SAGA and ATAC histone acetyl transferase complexes regulate distinct sets of genes and ATAC defines a class of p300-independent enhancers. *Mol. Cell*, **44**, 410–423.
19. Hirsch,C., Coban Akdemir,Z., Wang,L., Jayakumaran,G., Trcka,D., Weiss,A., Hernandez,J., Pan,Q., Han,H., Xu,X. *et al.* (2015) Myc and SAGA rewire an alternative splicing network during early somatic cell reprogramming. *Genes Dev.*, **29**, 803–816.
20. Vorobyeva,N.E., Mazina,M.U., Golovnin,A.K., Kopytova,D.V., Gurskiy,D.Y., Nabirochkina,E.N., Georgieva,S.G., Georgiev,P.G. and Krasnov,A.N. (2013) Insulator protein Su(Hw) recruits SAGA and Brahma complexes and constitutes part of Origin Recognition Complex-binding sites in the Drosophila genome. *Nucleic Acids Res.*, **41**, 5717–5730.
21. Bohla,D., Herold,M., Panzer,I., Buxa,M.K., Ali,T., Demmers,J., Kruger,M., Scharfe,M., Jarek,M., Bartkuhn,M. *et al.* (2014) A functional insulator screen identifies NURF and dREAM components to be required for enhancer-blocking. *PLoS One*, **9**, e107765.
22. Nelson,J.D., Denisenko,O. and Bomsztyk,K. (2006) Protocol for the fast chromatin immunoprecipitation (ChIP) method. *Nat. Protoc.*, **1**, 179–185.
23. Langmead,B., Trapnell,C., Pop,M. and Salzberg,S.L. (2009) Ultrafast and memory-efficient alignment of short DNA sequences to the human genome. *Genome Biol.*, **10**, R25.
24. Feng,J., Liu,T. and Zhang,Y. (2011) Using MACS to identify peaks from ChIP-Seq data. *Curr. Protoc. Bioinformatics*, doi:10.1002/0471250953.bi0214s34.
25. Heinz,S., Benner,C., Spann,N., Bertolino,E., Lin,Y.C., Laslo,P., Cheng,J.X., Murre,C., Singh,H. and Glass,C.K. (2010) Simple combinations of lineage-determining transcription factors prime cis-regulatory elements required for macrophage and B cell identities. *Mol. Cell*, **38**, 576–589.
26. Huber,W., Carey,V.J., Gentleman,R., Anders,S., Carlson,M., Carvalho,B.S., Bravo,H.C., Davis,S., Gatto,L., Girke,T. *et al.* (2015) Orchestrating high-throughput genomic analysis with Bioconductor. *Nat. Methods*, **12**, 115–121.
27. Lawrence,M., Huber,W., Pages,H., Aboyoun,P., Carlson,M., Gentleman,R., Morgan,M.T. and Carey,V.J. (2013) Software for computing and annotating genomic ranges. *PLoS Comput. Biol.*, **9**, e1003118.
28. Morgan,M., Pagès,H., Obenchain,V. and Hayden,N. (2016) Rsamtools: binary alignment (BAM), FASTA, variant call (BCF), and tabix file import. *R package version 1.24.0*.
29. Love,M.I., Huber,W. and Anders,S. (2014) Moderated estimation of fold change and dispersion for RNA-seq data with DESeq2. *Genome Biol.*, **15**, 550.
30. Ye,T., Krebs,A.R., Choukrallah,M.A., Keime,C., Plewniak,F., Davidson,I. and Tora,L. (2011) seqMINER: an integrated ChIP-seq data interpretation platform. *Nucleic Acids Res.*, **39**, e35.
31. Shen,L., Shao,N., Liu,X. and Nestler,E. (2014) ngs.plot: Quick mining and visualization of next-generation sequencing data by integrating genomic databases. *BMC Genomics*, **15**, 284.
32. R-Development-Core-Team. (2008) R: A Language and Environment for Statistical Computing. *R Foundation for Statistical Computing*. Vienna.
33. Hahne,F. and Ivanek,R. (2016) Visualizing genomic data using Gviz and bioconductor. *Methods Mol. Biol.*, **1418**, 335–351.
34. Ong,C.T., Van Bortle,K., Ramos,E. and Corces,V.G. (2013) Poly(ADP-ribosyl)ation regulates insulator function and intrachromosomal interactions in Drosophila. *Cell*, **155**, 148–159.
35. Shevchenko,A., Tomas,H., Havlis,J., Olsen,J.V. and Mann,M. (2006) In-gel digestion for mass spectrometric characterization of proteins and proteomes. *Nat. Protoc.*, **1**, 2856–2860.
36. Trapnell,C., Roberts,A., Goff,L., Pertea,G., Kim,D., Kelley,D.R., Pimentel,H., Salzberg,S.L., Rinn,J.L. and Pachter,L. (2012) Differential gene and transcript expression analysis of RNA-seq experiments with TopHat and Cufflinks. *Nat. Protoc.*, **7**, 562–578.
37. Shen,L. (2013) GeneOverlap: test and visualize gene overlaps. *R package version 1.8.0*.
38. Weake,V.M. and Workman,J.L. (2012) SAGA function in tissue-specific gene expression. *Trends Cell Biol.*, **22**, 177–184.
39. Hochheimer,A., Zhou,S., Zheng,S., Holmes,M. and Tjian,R. (2002) TRF2 associates with DREF and directs promoter-selective gene expression in Drosophila. *Nature*, **420**, 439–445.
40. Gurudatta,B.V., Yang,J., Van Bortle,K., Donlin-Asp,P.G. and Corces,V.G. (2013) Dynamic changes in the genomic localization of DNA replication-related element binding factor during the cell cycle. *Cell Cycle*, **12**, 1605–1615.
41. Heseding,C., Saumweber,H., Rathke,C. and Ehrenhofer-Murray,A.E. (2016) Widespread colocalization of the Drosophila histone acetyltransferase homolog MYST5 with DREF and insulator proteins at active genes. *Chromosoma*, doi:10.1007/s00412-016-0582-9.
42. Schwartz,Y.B., Linder-Basso,D., Kharchenko,P.V., Tolstorukov,M.Y., Kim,M., Li,H.B., Gorchakov,A.A., Minoda,A., Shanower,G., Alekseyenko,A.A. *et al.* (2012) Nature and function of insulator protein binding sites in the Drosophila genome. *Genome Res.*, **22**, 2188–2198.
43. Wood,A.M., Van Bortle,K., Ramos,E., Takenaka,N., Rohrbaugh,M., Jones,B.C., Jones,K.C. and Corces,V.G. (2011) Regulation of chromatin organization and inducible gene expression by a Drosophila insulator. *Mol. Cell*, **44**, 29–38.
44. Carré,C., Ciurciu,A., Komonyi,O., Jacquier,C., Fagegaltier,D., Pidoux,J., Tricoire,H., Tora,L., Boros,I.M. and Antoniewski,C. (2008) The Drosophila NURF remodelling and the ATAC histone acetylase complexes functionally interact and are required for global chromosome organization. *EMBO Rep.*, **9**, 187–192.
45. Fujioka,M., Wu,X. and Jaynes,J.B. (2009) A chromatin insulator mediates transgene homing and very long-range enhancer-promoter communication. *Development*, **136**, 3077–3087.
46. Fujioka,M., Mistry,H., Schedl,P. and Jaynes,J. (2016) Determinants of Chromosome Architecture: Insulator Pairing in cis and in trans. *PLoS Genet.*, **12**, e1005889.
47. Fujioka,M., Sun,G. and Jaynes,J.B. (2013) The Drosophila eve insulator Homie promotes eve expression and protects the adjacent gene from repression by polycomb spreading. *PLoS Genet.*, **9**, e1003883.
48. Nishimasu,H., Ran,F.A., Hsu,P.D., Konermann,S., Shehata,S.I., Dohmae,N., Ishitani,R., Zhang,F. and Nureki,O. (2014) Crystal structure of Cas9 in complex with guide RNA and target DNA. *Cell*, **156**, 935–949.
49. Liang,J., Lacroix,L., Gamot,A., Cuddapah,S., Queille,S., Lhoumaud,P., Lepetit,P., Martin,P.G., Vogelmann,J., Court,F. *et al.* (2014) Chromatin immunoprecipitation indirect peaks highlight long-range interactions of insulator proteins and Pol II pausing. *Mol. Cell*, **53**, 672–681.
50. Vogelmann,J., Le Gall,A., Dejardin,S., Allemand,F., Gamot,A., Labesse,G., Cuvier,O., Negre,N., Cohen-Gonsaud,M., Margeat,E. *et al.* (2014) Chromatin insulator factors involved in long-range DNA interactions and their role in the folding of the Drosophila genome. *PLoS Genet.*, **10**, e1004544.
51. Mohan,R.D., Workman,J.L. and Abmayr,S.M. (2014) Drosophila models reveal novel insights into mechanisms underlying neurodegeneration. *Fly (Austin)*, **8**, 148–152.
52. Kurshakova,M., Maksimenko,O., Golovnin,A., Pulina,M., Georgieva,S., Georgiev,P. and Krasnov,A. (2007) Evolutionarily conserved E(y)2/Sus1 protein is essential for the barrier activity of Su(Hw)-dependent insulators in Drosophila. *Mol. Cell*, **27**, 332–338.
53. Maksimenko,O., Kyrchanova,O., Bonchuk,A., Stakhov,V., Parshikov,A. and Georgiev,P. (2014) Highly conserved ENY2/Sus1 protein binds to Drosophila CTCF and is required for barrier activity. *Epigenetics*, **9**, 1261–1270.
54. Jin,Q., Zhuang,L., Lai,B., Wang,C., Li,W., Dolan,B., Lu,Y., Wang,Z., Zhao,K., Peng,W. *et al.* (2014) Gcn5 and PCAF negatively regulate

interferon-beta production through HAT-independent inhibition of TBK1. *EMBO Rep.*, **15**, 1192–1201.
55. Eaton,M.L., Prinz,J.A., MacAlpine,H.K., Tretyakov,G., Kharchenko,P.V. and MacAlpine,D.M. (2011) Chromatin signatures of the Drosophila replication program. *Genome Res.*, **21**, 164–174.
56. MacAlpine,H.K., Gordan,R., Powell,S.K., Hartemink,A.J. and MacAlpine,D.M. (2010) Drosophila ORC localizes to open chromatin and marks sites of cohesin complex loading. *Genome Res.*, **20**, 201–211.
57. Feller,C., Forne,I., Imhof,A. and Becker,P.B. (2015) Global and specific responses of the histone acetylome to systematic perturbation. *Mol. Cell*, **57**, 559–571.
58. Venkatesh,S. and Workman,J.L. (2015) Histone exchange, chromatin structure and the regulation of transcription. *Nat. Rev. Mol. Cell Biol.*, **16**, 178–189.
59. Qiu,H., Chereji,R.V., Hu,C., Cole,H.A., Rawal,Y., Clark,D.J. and Hinnebusch,A.G. (2015) Genome-wide cooperation by HAT Gcn5, remodeler SWI/SNF, and chaperone Ydj1 in promoter nucleosome eviction and transcriptional activation. *Genome Res.*
60. Govind,C.K., Zhang,F., Qiu,H., Hofmeyer,K. and Hinnebusch,A.G. (2007) Gcn5 promotes acetylation, eviction, and methylation of nucleosomes in transcribed coding regions. *Mol. Cell*, **25**, 31–42.
61. Ahanger,S.H., Gunther,K., Weth,O., Bartkuhn,M., Bhonde,R.R., Shouche,Y.S. and Renkawitz,R. (2014) Ectopically tethered CP190 induces large-scale chromatin decondensation. *Sci. Rep.*, **4**, 3917.
62. Kwon,S.Y., Grisan,V., Jang,B., Herbert,J. and Badenhorst,P. (2016) Genome-wide mapping targets of the metazoan chromatin remodeling factor NURF reveals nucleosome remodeling at enhancers, core promoters and gene insulators. *PLoS Genet.*, **12**, e1005969.
63. Lhoumaud,P., Hennion,M., Gamot,A., Cuddapah,S., Queille,S., Liang,J., Micas,G., Morillon,P., Urbach,S., Bouchez,O. *et al.* (2014) Insulators recruit histone methyltransferase dMes4 to regulate chromatin of flanking genes. *EMBO J.*, **33**, 1599–1613.